DRAFT VERSION APRIL 8, 2016
Preprint typeset using LaTeX style emulateapj v. 5/2/11

arXiv:1602.05892v2 [astro-ph.SR] 6 Apr 2016

THE SOLAR INTERNETWORK. II. MAGNETIC FLUX APPEARANCE AND DISAPPEARANCE RATES

M. GOŠIĆ[1], L. R. BELLOT RUBIO[1], J. C. DEL TORO INIESTA[1], D. OROZCO SUÁREZ[2], AND Y. KATSUKAWA[3]
[1] Instituto de Astrofísica de Andalucía (CSIC), Apdo. 3004, E-18080 Granada, Spain; mgosic@iaa.es
[2]Instituto de Astrofísica de Canarias, E-38205 La Laguna, Tenerife, Spain and
[3] National Astronomical Observatory of Japan, 2-21-1 Osawa, Mitaka, Tokyo 181-8588, Japan
Draft version April 8, 2016

ABSTRACT

Small-scale internetwork magnetic fields are important ingredients of the quiet Sun. In this paper we analyze how they appear and disappear on the solar surface. Using high resolution *Hinode* magnetograms, we follow the evolution of individual magnetic elements in the interior of two supergranular cells at the disk center. From up to 38 hr of continuous measurements, we show that magnetic flux appears in internetwork regions at a rate of 120 ± 3 Mx cm^{-2} day^{-1} ($3.7 \pm 0.4 \times 10^{24}$ Mx day^{-1} over the entire solar surface). Flux disappears from the internetwork at a rate of 125 ± 6 Mx cm^{-2} day^{-1} ($3.9 \pm 0.5 \times 10^{24}$ Mx day^{-1}) through fading of magnetic elements, cancellation between opposite-polarity features, and interactions with network patches, which converts internetwork elements into network features. Most of the flux is lost through fading and interactions with the network, at nearly the same rate of about 50 Mx cm^{-2} day^{-1}. Our results demonstrate that the sources and sinks of internetwork magnetic flux are well balanced. Using the instantaneous flux appearance and disappearance rates, we successfully reproduce the time evolution of the total unsigned flux in the two supergranular cells.

Subject headings: Sun: magnetic field – Sun: photosphere

1. INTRODUCTION

Internetwork (IN) magnetic fields are observed to fill the interior of supergranular cells, enclosed by the photospheric network (NE). In Paper I of this series (Gošić et al. 2014) we showed that IN regions harbor some 10^{23} Mx over the entire solar surface, which accounts for 15% of the total quiet Sun (NE+IN) flux. We also demonstrated that IN fields represent the main source of flux for the NE, capable of supplying as much flux as it contains in only about 10 hr. This renders the IN an essential contributor to the flux budget of the solar photosphere—and probably also to its energy budget (Trujillo Bueno et al. 2004).

IN regions show an enormous flux appearance rate. The values quoted in the literature range from 10^{24} Mx day^{-1} (Zirin 1987) to 3.8×10^{26} Mx day^{-1} (Zhou et al. 2013). All of them are significantly larger than the 6×10^{21} Mx day^{-1} brought to the surface by active regions during the maximum of the solar cycle (Schrijver & Harvey 1994). However, the published rates vary by more than 2 orders of magnitude, indicating that they are not well determined yet. Much of the difference is probably due to the methods used to derive them. For example, some authors rely on automatic tracking algorithms while others prefer a manual detection of magnetic elements. Both approaches are affected by uncertainties and/or subjectivity (e.g., DeForest et al. 2007). Differences in the spatial resolution, noise level, cadence, and duration of the observations may also lead to different results. Another source of disagreement is the fact that many estimates are based on fitting the observed flux distributions with power laws, rather than on following the evolution of individual elements. This method assumes constant appearance rates, but in reality we do not know if the flux appears at a constant rate or there are spatial and temporal variations across the solar surface.

To understand the flux balance of IN regions, we have to evaluate the processes by which flux is injected into and removed from the interior of supergranular cells. The IN gains flux through in-situ appearance of magnetic elements. Sometimes bipolar structures can be clearly identified, but most elements seem to appear as unipolar patches. On the other hand, flux is removed from the cell interior by fading (disappearance of features without obvious interactions with other elements) and cancellation (total or partial disappearance of features of opposite polarity as they come into close contact). Fading has been reported to be the dominant process, accounting for 83% of the flux removal in the quiet Sun (Lamb et al. 2013). These authors determined a flux disappearance rate of 2.4×10^{26} Mx day^{-1} over the entire solar surface, but they did not distinguish between NE and IN regions.

Another important sink of IN flux that has been neglected until now is conversion of IN features into NE elements. In Paper I we made the first steps to quantify this process, showing that 40% of the IN flux eventually interacts with NE elements and disappears from the supergranular cell. Flux transfer from the IN to the NE is therefore an essential ingredient to understand the flux balance of quiet Sun regions.

In this paper we determine the rates of the four processes mentioned above, namely in-situ appearance, fading, cancellation, and flux transfer to the NE. We focus on two well-defined supergranular cells and compute the instantaneous fluxes that appear and disappear in their interiors. The analysis is based on long-duration, high-cadence magnetogram sequences taken with the Narrowband Filter Imager (NFI; Tsuneta et al. 2008) on board *Hinode* (Kosugi et al. 2007). These data are perfectly suited to study the highly dynamical IN fields on temporal scales from minutes to days. The evolution of IN flux elements is followed using an automatic feature tracking algorithm and a new code developed to accurately resolve interactions between flux patches (Section 3). In this way we are able to compute, for the first time, the flux appearance and disappearance rates in individual supergranular cells and their variations with time (Section 4).

2. OBSERVATIONS AND DATA PROCESSING

The data used in this paper consist of two temporal sequences acquired with the *Hinode* NFI on 2010 January 20–

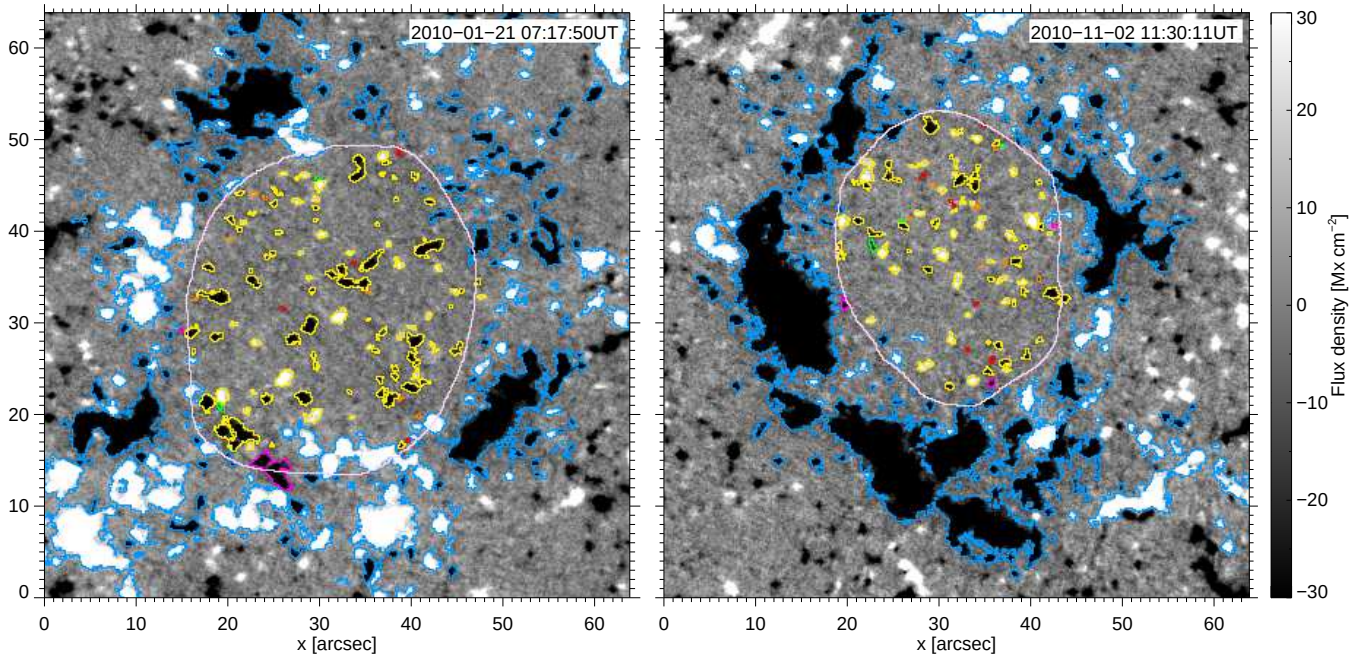

Figure 1. Individual supergranular cells observed in data sets 1 and 2 (left and right, respectively). The cell interiors are outlined by pink contours and the surrounding NE flux features are marked with blue contours. Red contours show IN elements that appear in situ in these frames. Magnetic flux disappears from the cell interiors when elements fade (orange), cancel out (green), or enter the NE and interact with NE features (purple). IN patches that do not undergo any of those processes in the displayed frames are indicated with yellow contours.
An animation of the right panel is available.

21 and 2010 November 2–3 (data sets 1 and 2, respectively). They belong to *Hinode* Operation Plan 151. The observations have been described in detail in Paper I, so here we only summarize their main features. Magnetograms and Dopplergrams were constructed from Stokes *I* and *V* filtergrams taken at $\pm$16 pm from the center of the magnetically sensitive Na I 589.6 nm line. We observed both line wings to make the magnetograms as independent of Doppler shifts as possible. In addition, we pushed the sensitivity of the observations to a limit by operating the NFI in shutterless mode. This allowed us to reach a total exposure time of 6.4 s per magnetogram, resulting in a noise level of 6 Mx cm^{-2}. The noise was further reduced to 4 Mx cm^{-2} through application of a 3×3 Gaussian-type spatial smoothing kernel. Thanks to these choices, our magnetogram sequences are among the most sensitive ever obtained in the quiet Sun with a filter instrument.

To study the evolution of the solar IN we made continuous measurements for 20 hr in the case of data set 1 and 38 hr in the case of data set 2. The sequences show a few gaps due to telemetry problems, but their duration is often short (of the order of minutes). The achieved cadences—60 and 90 s—are ideal for automatic tracking of magnetic features.

The observations cover large areas of the quiet Sun at disk center ($82'' \times 113''$ and $80'' \times 74''$, respectively). Solar rotation was compensated, making it possible to monitor individual supergranular cells for long periods of time. Here we focus on two cells that were visible at the center of the field of view during the entire sequences (Figure 1). They show an average total (NE+IN) unsigned flux of 2.4×10^{20} Mx and 3.6×10^{20} Mx, respectively. We observed their evolution from the early formation phases until they fully developed into mature cells. Their effective radius increased from $\sim$9.7 to $\sim$13 Mm during the process. Neither of them underwent mergings or fragmentations. Thanks to the longer duration of the second data set, we witness how the supergranule disperses with time and slowly loses its form, although it is still visible by the end of the observations. This cell is strongly unipolar and shows a net flux of -2.3×10^{20} Mx (enhanced NE). By contrast, the supergranular cell of data set 1 is in almost perfect polarity balance with a net flux of -2×10^{18} Mx (quiet NE).

3. METHOD

Our goal is to determine the instantaneous flux appearance and disappearance rates in the two supergranular cells described above. This requires us to detect and track all the individual magnetic elements visible in their interiors. As explained in Paper I, the cell boundaries are known precisely from horizontal flow divergence maps derived from the available Dopplergrams through Local Correlation Tracking (November & Simon 1988), and turn out to be pretty well outlined by the strong patches of the NE.

We use the YAFTA code (Welsch & Longcope 2003) and the clumping method to automatically identify and track individual elements in the magnetogram sequences. Only features that have at least 4 pixels with flux densities above 12 Mx cm^{-2} (three times the noise level) and live for 2 or more frames are taken into consideration. We have developed a new code to solve some of the problems that lead to misidentifications and/or incorrect labeling of the magnetic elements (Gošić et al., in preparation). By use of this code we can follow individual elements from birth to death, which is necessary to derive reliable appearance and disappearance rates. The quality of the final tracking can be assessed from the animation accompanying Figure 1.

Supergranular cells gain flux through in-situ appearance of magnetic elements and their subsequent evolution. The flux

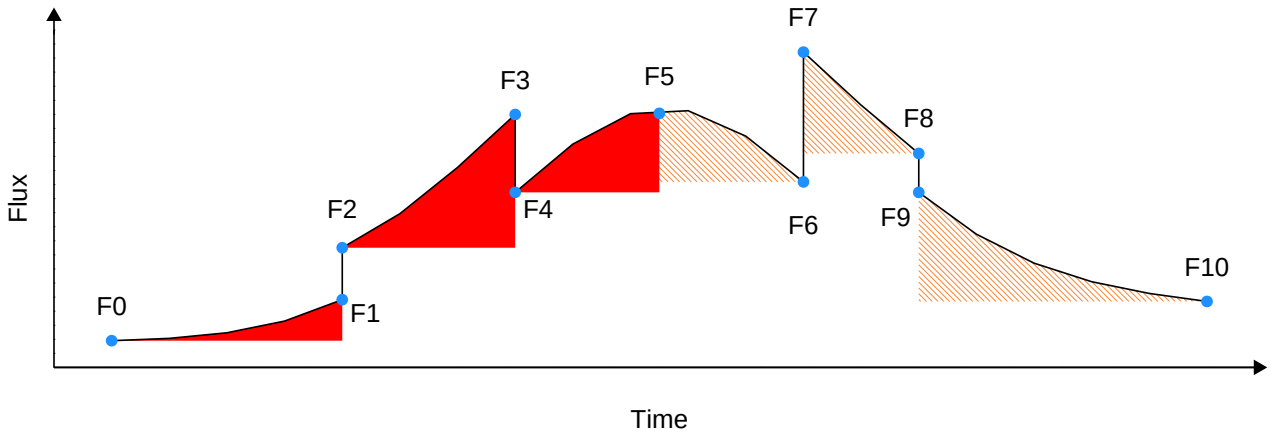

Figure 2. Sketch of the flux evolution of typical IN magnetic elements. The red shaded areas represent the flux gained by an element during its lifetime. The orange shaded areas represent the flux lost by fading until the element disappears (by either in-situ fading, cancellation, or merging with a stronger flux patch). Blue dots mark the moments of appearance, disappearance, and interactions.

contributed by an element to the IN is not only its initial flux, but also any intrinsic flux increase it may experience with time. We refer to the sum of both contributions as total appeared flux. Flux disappears from the cell when IN elements fade inside the supergranule, cancel totally or partially with opposite-polarity IN elements, or leave the supergranule and interact with NE elements (a process we refer to as flux transfer to the NE). Below we explain how the rates of these processes are calculated and describe the problems solved by our code in each case.

3.1. *Flux sources*

The flux that appears in situ in a given frame is computed considering all IN patches that become visible for the first time in that frame. Identifying those elements is easy because YAFTA tags them with new labels. If the elements do not interact with other patches, their maximum flux is taken to be the flux they bring to the solar surface. IN elements tend to increase in flux upon appearance, so the maximum flux they reach is usually larger than the initial one. When interactions occur, however, the maximum flux is not a good indicator of the flux appearing on the surface, because the elements may simply grow through mergings with like-polarity patches. The flux gained in this way does not represent new flux and should not be counted. In addition, elements that appear in situ can fragment a few frames later and the fragments themselves may continue to gain flux. Such a flux increase needs to be added to the flux appearance rate. Fragments are tagged by YAFTA as children of their parents, so they are easy to detect.

Thus, one has to be careful with interactions to derive reliable flux appearance rates. In practice, we go through each of the magnetic elements assigned a new label by YAFTA in a given frame—either because they appeared in situ or because they fragmented from an existing element. We examine how they gain flux over time, correct for mergings and fragmentations, and sum all the contributions to get the total flux they bring to the surface. The process is illustrated schematically in Figure 2. The solid line represents the flux of an IN element during its evolution. The moments of appearance, disappearance, and interactions are marked with dots. Each dot has a value from $F0$ to $F10$, which corresponds to the flux of the element at those particular times. $F2$ and $F7$ coincide with sudden flux increases due to mergings with weaker elements. The maximum observed flux is $F7$, but this value is the result of one such merging. $F5$ would be the maximum flux in the absence of interactions. There are two fragmentations which decrease the flux from $F3$ to $F4$ and from $F8$ to $F9$, respectively.

We calculate the total flux the element brings to the supergranular cell by adding together the initial flux $F_{\rm init}$ and the flux increases from one checkpoint to the next (blue dots), i.e.,

$$F_{\rm app} = F_{\rm init} + (F1 - F0) + (F3 - F2) + (F5 - F4). \quad (1)$$

If the element appeared in situ, we take $F_{\rm init} = F0$. If it is a fragment of an existing patch, then $F_{\rm init} = 0$. The flux $F_{\rm init}$ is assigned to the moment when the element was first detected (also for fragments). The other contributions in Equation 1 are evenly distributed over their corresponding time intervals.

By adding the flux carried by the patches that appear in situ and through fragmentation we obtain the total flux appearance rate. For completeness, we also compute the appearance rate using only the initial flux of the features that appear in situ. We do this because the initial flux is a well-defined quantity that does not depend on interactions between patches. This rate represents the flux that discrete magnetic elements bring to the solar IN right at the moment of appearance, before they experience any perturbation.

It should be clear by now that a very accurate tracking of magnetic elements is mandatory to obtain reliable flux appearance rates. In particular, false detections of disappearances followed by appearances of the same element must be avoided. This problem occurs frequently due to fluctuations in the signal of the elements. They may exhibit flux densities below the detection threshold during a few frames, only to return to their previous state after such episodes. YAFTA interprets this evolution as the disappearance of the element by fading and the subsequent appearance of a new like-polarity patch at the same location, artificially increasing the appearance and disappearance rates. Our code corrects for this problem in the following way.

For each element disappearing in situ, we check whether a new like-polarity flux structure appears nearby in the next three frames. In that case, the new patch is considered to be the evolution of the previously disappeared element if three conditions are met. First, the newly appeared element has to have at least 30% of its area inside a circle centered on the

flux-weighted center of the disappeared element. The circle radius is 2 pixels (230 km) in the frame after the disappearance occurred, and 4 pixels afterward. Second, the size and total flux of the two patches cannot differ by more than a factor of three. Third, if any of the two elements is visible in only one frame, then they have to overlap by more than 70%. This correction decreases both the flux appearance and disappearance rates by 10%, compared with the original YAFTA results.

Another problem fixed by our code is in-situ appearance of IN elements followed by merging with existing NE patches in the same frame. YAFTA does not detect these IN features and therefore their flux is not included in the flux appearance rates. We identify such elements by comparing the shapes of the NE elements that are inside the cell with the shapes they had in the previous frame, looking for large size changes. When we find 16 or more contiguous pixels in the non-overlapping area, they are taken to be a newly appeared IN element which merged with the NE patch right away. In our data sets, such a correction increases the appearance rates by approximately 5%. Yet, this is only a lower limit because structures smaller than 16 pixels are not counted in (to avoid errors induced by the intrinsic shape variation of NE patches from frame to frame).

3.2. *Flux sinks*

The simplest process of flux disappearance from supergranules is in-situ fading, whereby IN magnetic elements disappear in a given frame without interacting with other features in their vicinity. YAFTA tags fading events as in-situ disappearances, so their detection is relatively straightforward (but see below). The flux they remove from the IN is calculated in a similar way as the flux that appears on the solar surface. If the element does not undergo interactions, the total flux lost by fading is the maximum flux it attains during its lifetime. When interactions occur, we determine how the flux decreases from one interaction to the next. In the example of Figure 2, the total flux removed by fading is

$$F_{\rm fading} = (F5 - F6) + (F7 - F8) + (F9 - F10) + F_{\rm final}. \qquad (2)$$

$F_{\rm final} = F10$ if the element disappears completely by fading. If the patch loses its label at $F10$ because of a merging with a stronger feature (either from the IN or from the NE), then $F_{\rm final} = 0$ to avoid counting the flux it had right before the merging. Thus, even though mergings do not remove flux from the photosphere, we still calculate the flux lost by fading before the elements merge with stronger features. The flux $F_{\rm final}$ is assigned to the frame where the element is detected for the last time, and the remaining terms to their respective intervals.

The second mechanism capable of removing flux from the IN is cancellation of opposite-polarity patches. It turns out that YAFTA does not identify this as a process different from in-situ disappearance. To detect cancellations, we use the YAFTA output and look for IN elements that disappear at most 2 pixels away from an opposite-polarity IN patch. The flux lost by the supergranular cell through this process is equal to the flux the two canceling features had at the beginning of the cancellation. If the magnetic elements merge with other patches or fragment during the process, we keep track of the changes and revise the total canceled flux accordingly. In partial cancellations with one surviving feature, the canceled flux is taken to be twice the flux of the feature that disappeared completely. Partial cancellations where neither of the elements disappear are very difficult to detect, so we do not account for them. As a consequence, our flux cancellation rates may be smaller than the actual ones. However, the total disappearance rate is correct, because the flux removed in those cases is counted as fading flux. For all the magnetic elements that cancel out, we check if they lose flux before the cancellation starts. Any observed flux drop is ascribed to fading.

The third mechanism of flux removal from the IN is transfer to the NE. Many IN elements are sufficiently persistent to drift toward the supergranular border (e.g., Orozco Suárez et al. 2012), where they merge or cancel with NE patches. In both cases, the IN loses flux. This complex process has been characterized in Paper I. The basic idea is to follow the evolution of all IN flux structures to determine if they interact with NE patches. The flux lost by the IN is taken to be the flux of the IN element in the frame before the merging or cancellation occurred. More details about these calculations are provided in Paper I.

Finally, we note that the IN flux our code detects to appear in situ and immediately merge with NE features is counted also as IN flux transferred to the NE, which increases the total flux disappearance rate by almost 5% compared with the plain YAFTA results.

3.3. *Uncertainties*

The main source of error in the YAFTA tracking is the misidentification of magnetic elements that fade and reappear again. As explained above, the method we use to correct for this problem depends on a number of (free) parameters such as circle radius, minimum area overlap, and maximum flux and size variations. These parameters have been adjusted manually to yield the best possible results, but of course they introduce uncertainties in the flux appearance and disappearance rates. In what follows we estimate them.

We use two limiting cases. The first case represents the plain YAFTA results. Here, many magnetic features are erroneously identified as new elements when their fluxes drop below and later rise above the 3σ level.

The other limiting case is computed using only one parameter, namely the radius of the circle in which we look for reappearing elements. If a new magnetic feature shows up inside or touches the border of a circle of radius 4 pixels, then that feature is considered to be the continuation of the previously disappeared element, regardless of its flux or size. This criterion is too lax, producing bad identifications of many elements that are detected as reoccurring patches. The appearance and disappearance rates in this extreme case are 23% and 19% lower than those from the non-corrected YAFTA output, respectively.

The combination of parameters we actually use in the analysis leads to more strict criteria for the identification of these elements. Thus, our final appearance and disappearance rates are 10% lower than those obtained with the plain YAFTA tracking, and 13%-9% larger than those resulting from the second limiting case. Therefore, an upper limit for the uncertainty caused by the choice of parameters is $\pm$13% (appearance rate) and $\pm$10% (disappearance rate).

4. RESULTS

Figure 3 displays the rates at which the IN gains and loses flux in the supergranular cell of data set 1. The data points are binned in 30 minute intervals.

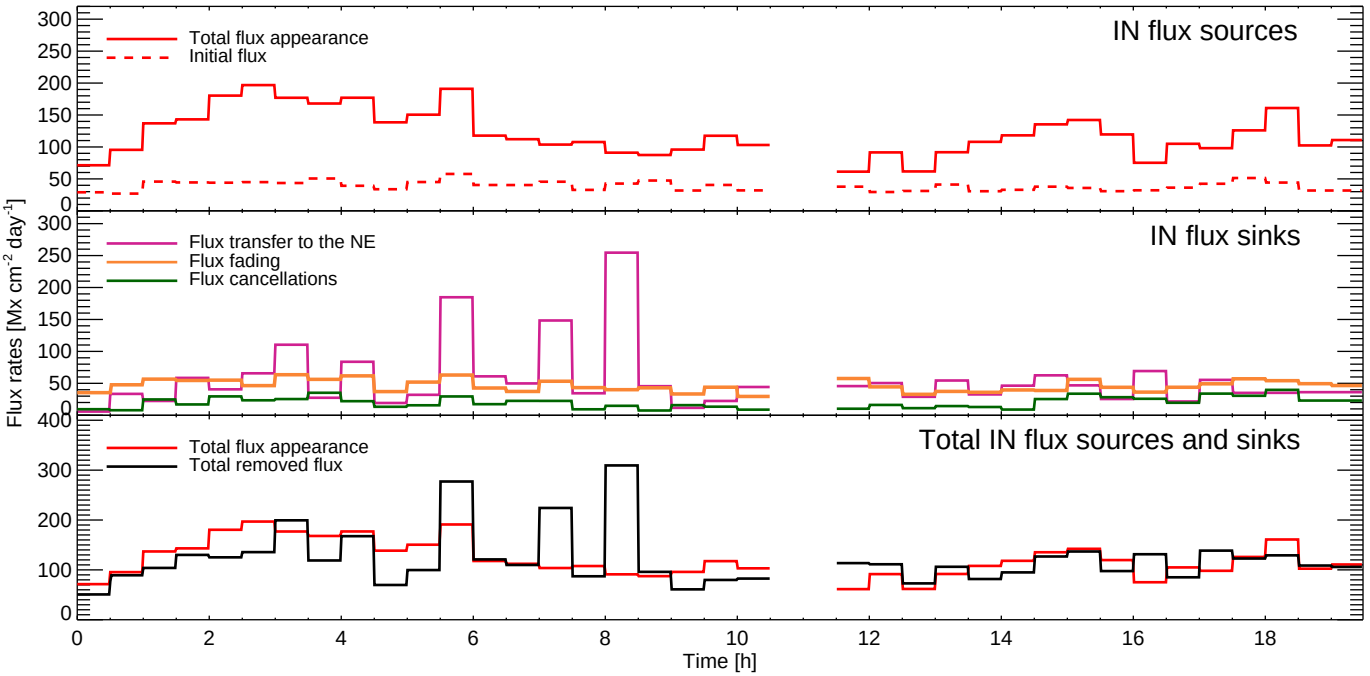

Figure 3. Rates at which the central supergranule of data set 1 gains and loses magnetic flux. The data are binned in 30 minute intervals. Top panel: the source of IN flux is in-situ appearance of magnetic features and their subsequent evolution (red solid curve). The red dashed line shows the initial flux of the elements that appear in situ. Middle panel: flux is removed from the cell by three mechanisms, namely interaction of IN patches with NE elements (flux transfer to the NE; purple), in-situ disappearance of magnetic elements (orange), and cancellation of IN features (green). Bottom panel: total rates at which flux is accumulated (red solid line) and removed (black solid line) from the cell. The latter is defined as the sum of the flux sinks displayed in the middle panel.

The top panel shows the total flux appearance rate as a function of time (solid line). On average, newly appeared features bring 117 Mx cm^{-2} day^{-1} to the surface. The appearance rate increases when strong magnetic elements pop up in the interior of the cell in the form of clusters. This is what happened, for example, between 1 and 6 hr. During that interval, the instantaneous appearance rate nearly doubled, reaching $\sim$200 Mx cm^{-2} day^{-1}. The flux appearance rate computed using the initial flux of the elements is 38 Mx cm^{-2} day^{-1}, with very little fluctuations (dashed line).

The middle panel of Figure 3 shows the flux removed from the cell by interactions with NE patches (purple curve), fading (orange curve), and cancellations (green curve). Transfer of magnetic elements from the IN to the NE turns out to be a very important process of flux disappearance from the supergranule, at an average rate of 53 Mx cm^{-2} day^{-1}. This process shows large temporal variations in the selected cell. The peaks between 6 and 8 hr, for example, were produced by strong patches leaving the IN and merging with the NE. In addition to this mechanism, flux disappears from the supergranule through fading, at a rate of 46 Mx cm^{-2} day^{-1}, and through cancellations, at a rate of 20 Mx cm^{-2} day^{-1}. Thus, fading and transfer to the NE are equally important sinks of flux for this cell, with cancellations playing a secondary role.

The sources and sinks of magnetic flux are shown in the bottom panel of Figure 3 with red and black lines, respectively. As can be seen, the flux appearance and removal rates are similar, but their peaks do not coincide exactly. The reason is that magnetic elements grow in flux upon appearance, reach their maximum, and disappear at a later time, depending on their intrinsic evolution and the interactions they undergo.

Figure 4 summarizes the results for the supergranular cell of data set 2. We observe an average total flux appearance rate of 122 Mx cm^{-2} day^{-1}. Fluctuations occur when clusters of magnetic patches appear in the cell interior. They can be seen at around 10 and 18 hr, for example. By contrast, the initial flux appearance rate is very stable at 41 Mx cm^{-2} day^{-1}.

Also in this case, transfer of IN flux to the NE and fading are the main flux removal mechanisms (second panel of Figure 4). The rates at which the cell loses flux through interactions with the NE is 47 Mx cm^{-2} day^{-1}. Fading is slightly larger, accounting for 59 Mx cm^{-2} day^{-1}, while cancellations proceed at a rate of 25 Mx cm^{-2} day^{-1}. In general, IN patches that convert into NE elements are small, but occasionally we detect strong IN features carrying much flux away from the cell interior. These events are easily distinguishable at, e.g., the beginning of the time sequence or 18 hr. The cancellation rates are smaller but more stable than the flux transfer to the NE.

Just like in data set 1, the supergranular cell of data set 2 gains and loses flux at nearly the same rate (Figure 4, bottom panel).

5. DISCUSSION

Our results convey information on and have implications for the flux balance of IN regions, the magnetic flux history of supergranular cells, and the mechanisms responsible for the appearance of flux on the solar surface. We discuss these implications in the following.

5.1. *Flux appearance and disappearance rates in the IN*

Table 1 summarizes the average appearance and disappearance rates obtained from the analysis of the *Hinode*/NFI observations, along with their ratio. As can be seen, magnetic

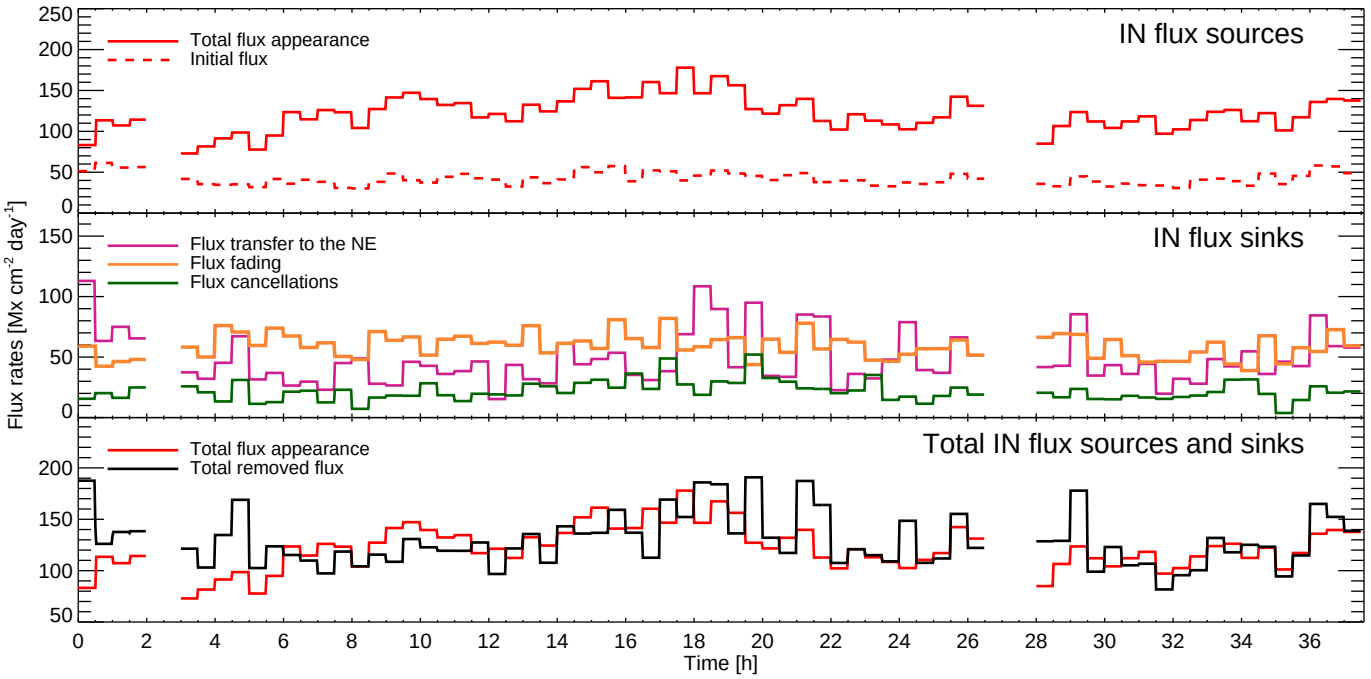

Figure 4. Same as Figure 3, for the central supergranule of data set 2.

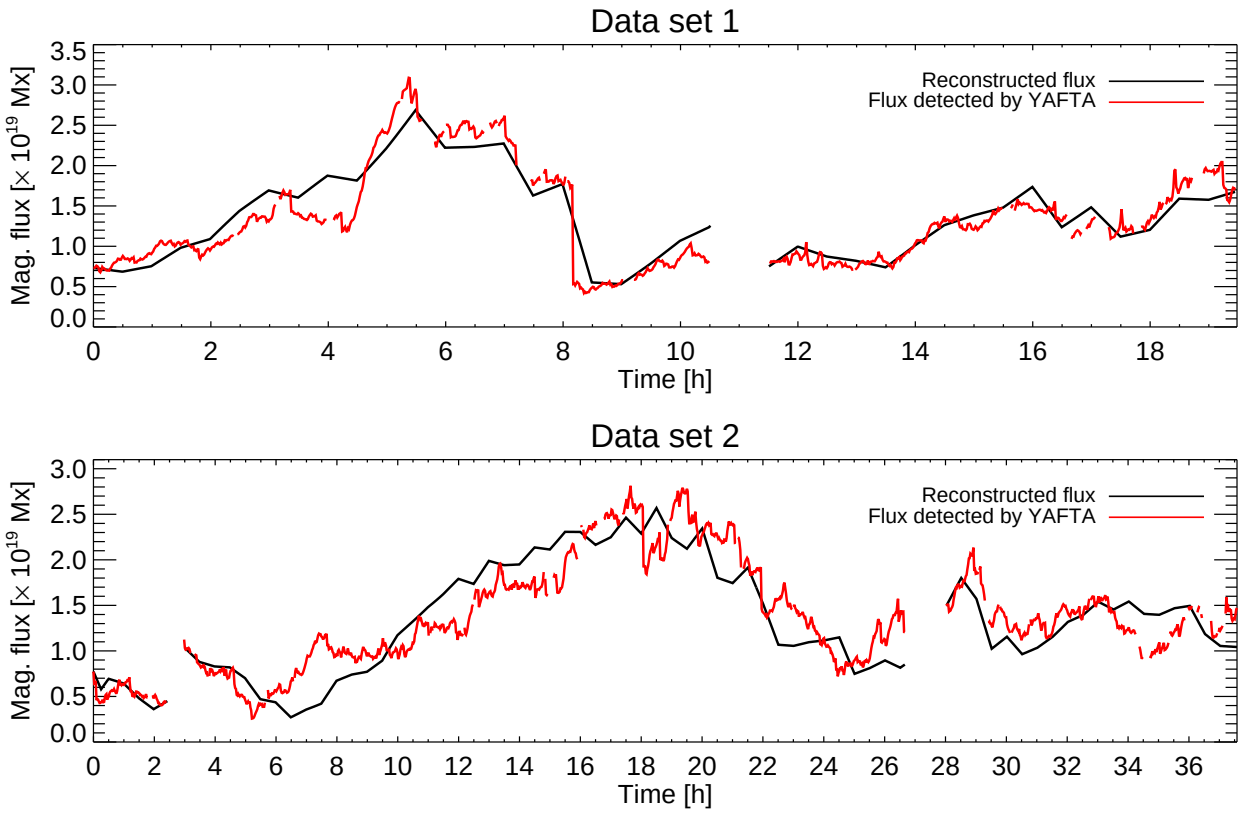

Figure 5. Comparison between the total unsigned flux observed in the central supergranular cells of data sets 1 (top) and 2 (bottom) and the flux reconstructed using the instantaneous appearance and disappearance rates.

Table 1
IN flux appearance and disappearance rates (Mx cm^{-2} day^{-1})

	Data Set 1	Data Set 2	Mean
Appearance			
In-situ	117	122	120 ± 3
Disappearance			
Fading	46	59	53 ± 7
Cancellation	20	25	23 ± 3
Transfer to NE	53	47	50 ± 3
Total	119	131	125 ± 6
Disappearance/Appearance	1.02	1.07	1.04 ± 0.03

flux appears in the IN at a rate of 120 ± 3 Mx cm^{-2} day^{-1} (40 ± 1 Mx cm^{-2} day^{-1} if the initial flux of the magnetic elements is considered). The total flux appearance rate is nearly the same in the two individual supergranular cells studied here, but it changes significantly whenever clusters of magnetic elements emerge into the surface. At those moments, the instantaneous rates can be as large as 200 Mx cm^{-2} day^{-1}.

Our total appearance rate implies that the flux brought to the entire solar surface by IN elements is 3.7×10^{24} Mx day^{-1} (because the IN occupies 47% and 54% of the FOV in data sets 1 and 2, respectively). This value is larger than the 3×10^{22} to 1.5×10^{24} Mx day^{-1} injected by bipolar ephemeral regions (Schrijver et al. 1997; Title 2000; Chae et al. 2001; Hagenaar 2001; Hagenaar et al. 2008), the 2.6×10^{24} Mx day^{-1} brought by horizontal IN fields (Lites et al. 1996), and the $\sim 10^{24}$ Mx day^{-1} carried by small-scale magnetic loops emerging in the solar IN (Zirin 1987; Martínez González & Bellot Rubio 2009). On the other hand, our rates are lower than the 3×10^{25} and 3.8×10^{26} Mx day^{-1} reported by Thornton & Parnell (2010) and Zhou et al. (2013), also based on *Hinode*/NFI measurements. Still, they are enormous.

The removal of flux from supergranular cells occurs mainly through interactions of IN features with NE patches and in-situ fading, at rates of 50 ± 3 and 53 ± 7 Mx cm^{-2} day^{-1}, respectively. These two mechanisms account for about 40% and 42% of the total flux lost by IN regions. The rest disappears by cancellation of IN elements, at a rate of 23 ± 3 Mx cm^{-2} day^{-1} which is nearly the same in the two supergranules we have studied.

The total disappearance rate implied by the three mechanisms capable of removing flux from the IN is similar to the rate at which the supergranules gain flux (see Table 1). They coincide to within 7%, reflecting the steady-state nature of the solar IN demonstrated by Figure 5 of Paper I. The small imbalance we observe is probably not real, but a result of our limited magnetic sensitivity and ability to interpret interactions between IN patches.

5.2. *Magnetic flux history of supergranular cells*

The instantaneous flux appearance and disappearance rates derived in the previous sections allow us to reproduce the temporal evolution of the flux in the interior of supergranular cells. Figure 5 shows a comparison between the total unsigned flux $F(t)$ observed in the supergranules of data sets 1 and 2 and the result of integrating the instantaneous rates over time as

$$F(t) = F(t_0) + \int_{t_0}^{t} [F_{\rm app}(t) - F_{\rm disapp}(t)]\, A(t)\, {\rm d}t, \qquad (3)$$

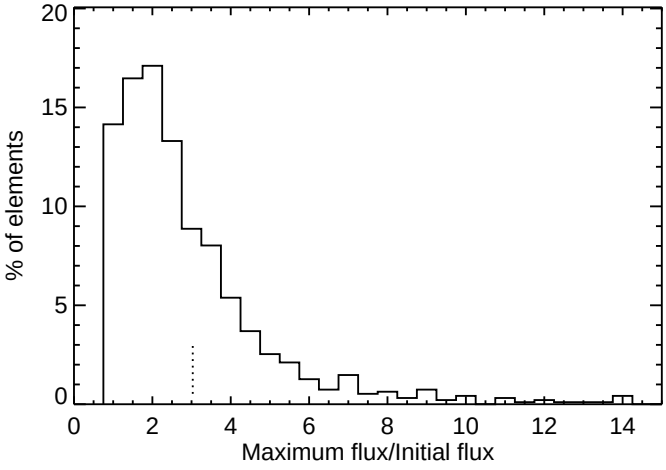

Figure 6. Histogram of the ratio between the maximum and the initial flux of the IN elements that appear in situ, live for at least 4 frames (6 minutes), and never interact with other elements in data set 2. The mean and median of the distribution are 3.0 and 2.4, respectively.

where $F(t_0)$ is the total unsigned flux in the cell at the beginning of the sequence, $F_{\rm app}(t)$ and $F_{\rm disapp}(t)$ are the appearance and disappearance rates displayed in Figures 3 and 4, and $A(t)$ is the area of the supergranular cell at time t.

The agreement is excellent and testifies to the precision and relevance of our results: for the first time, the evolution of IN flux is reproduced to a remarkable degree of accuracy.

5.3. *Origin of IN flux*

Comparing the total and initial flux appearance rates it is clear that magnetic elements grow in flux upon appearance. Indeed, the average initial flux of IN elements is 1.3×10^{16} Mx but, as can be seen in Figure 6, their maximum flux is on average three times larger. This has been determined using all IN elements that appear in situ, live for more than 6 minutes, and never interact with other features (Gošić 2012), so it is an intrinsic change. Such a flux increase explains why the ratio between the total and initial flux appearance rates is also about 3.

The fact that magnetic elements gain flux after their appearance is puzzling but may convey important information on the origin of the IN flux. One possibility is that the increase is simply due to continuous flux emergence on the surface. Another possibility is that the magnetic features are formed by coalescence of undetected background flux which is too weak to stand out above the noise level until sufficient flux has accumulated, as proposed by Lamb et al. (2008, 2010). This process may continue after the feature is first observed, increasing its flux. Changes in the magnetic field inclination, with the structures becoming more vertical with time, is another possible explanation for the flux increase detected in longitudinal magnetograms (Bellot Rubio & Orozco Suárez 2015). It is necessary to confirm whether or not these mechanisms operate on the solar surface and understand how they affect observations, because of their implications. For example, if a large fraction of the flux that appears in situ is due to coalescence and not to genuine bipolar emergence, then the actual amount of new flux brought to the surface may be significantly smaller than suggested by current analyses. In that case, part of the flux observed in supergranular cells would actually be recycled (network?) flux whose magnetic connec-

tivity is impossible to trace after substantial reprocessing.

To clarify these issues, we will investigate the modes of appearance and the properties of IN magnetic features—including their intrinsic increase of flux—in the next paper of this series.

The data used here were acquired in the framework of the *Hinode* Operation Plan 151 "*Flux replacement in the solar network and internetwork.*" We thank the *Hinode* Chief Observers for the efforts they made to accommodate our demanding observations. *Hinode* is a Japanese mission developed and launched by ISAS/JAXA, with NAOJ as a domestic partner and NASA and STFC (UK) as international partners. It is operated by these agencies in co-operation with ESA and NSC (Norway). MG acknowledges a JAE-Pre fellowship granted by Agencia Estatal Consejo Superior de Investigaciones Científicas (CSIC) toward the completion of a PhD degree. This work has been funded by the Spanish Ministerio de Economía y Competitividad through projects AYA2012-39636-C06-05 and ESP2013-47349-C6-1-R, including a percentage from European FEDER funds. Use of NASA's Astrophysical Data System is gratefully acknowledged.

REFERENCES

Bellot Rubio, L.R., & Orozco Suárez, D. 2015, Living Reviews in Solar Physics, in press
Chae, J., Martin, S. F., & Yun, H. S. et al. 2001, ApJ, 548, 497
DeForest, C. E., Hagenaar, H. J., & Lamb, D. A. et al. 2007, ApJ, 666, 576
Gošić, M. 2012, Master Thesis, University of Granada (Spain)
Gošić, M., Bellot Rubio, L.R., Orozco Suárez, D., Katsukawa, Y., and del Toro Iniesta, J.C. 2014, ApJ, 797, 49
Hagenaar, H. J. 2001, ApJ, 555, 448
Hagenaar, H. J., DeRosa, M. L., & Schrijver, C. J. 2008, ApJ, 678, 541
Kosugi, T., Matsuzaki, K., Sakao, T., et al. 2007, Sol. Phys., 243, 3
Lamb, D. A., DeForest, C. E., & Hagenaar, H., J. et al. 2008, ApJ, 674, 520
Lamb, D. A., DeForest, C. E., & Hagenaar, H., J. et al. 2010, ApJ, 720, 1405
Lamb, D. A., Howard, T. A., & DeForest, C. E. et al. 2013, ApJ, 774, 127
Lites, B. W., Leka, K. D., & Skumanich, A., et al. 1996, ApJ, 460, 1019
Martínez González, M. J., & Bellot Rubio, L. R. 2009, ApJ, 700, 1391
November, N., & Simon, W. G. 1998, ApJ, 333, 427
Orozco Suárez, D., Katsukawa, Y., & Bellot Rubio, L. R. 2012, ApJ, 758, L38
Schrijver, C. J., & Harvey, K. L. 1994, Sol. Phys., 150, 1
Schrijver, C. J., Title, A. M., & Hagenaar, H. J. et al. 1997, ApJ, 487, 424
Title, A. M. 2000, Philos. Trans. Roy. Soc. London A, 358, 657
Thornton, L. M., & Parnell, C. E. 2010, Sol. Phys., 269, 13
Trujillo Bueno, J., Shchukina, N., & Asensio Ramos, A. 2004, Nature, 430, 326
Tsuneta, S., Ichimoto, K., & Katsukawa, Y. 2008, Sol. Phys., 249, 167
Welsch, B. T., & Longcope, D. W. 2003, ApJ, 588, 620
Zhou, G., Wang, J., & Jin, C. 2013, Sol. Phys., 283, 273
Zirin, H. 1987, Sol. Phys., 110, 101